1 Systematic Entomology, School of Agriculture, Hokkaido University, Sapporo 060-8589, Japan; 2 Illinois Natural History Survey, University of Illinois, Champaign, Illinois 61820, USA

Wing base structure supports Coleorrhyncha + Auchenorrhyncha (Insecta: Hemiptera)

Kazunori Yoshizawa 1, Naoki Ogawa 1 and Christopher H. Dietrich 2

Corresponding author: Kazunori Yoshizawa (psocid@res.agr.hokudai.ac.jp)
Contributing authors: Naoki Ogawa (ogawa222@res.agr.hokudai.ac.jp), Christopher H. Dietrich (chdietri@illinois.edu)

Abstract

The phylogenetic placement of the moss bugs (Insecta: Hemiptera: Coleorrhyncha) has been highly controversial. Many apparent morphological apomorphies support the close relationship between Coleorrhyncha and Heteroptera (= true bugs). However, a recent phylogenomic study strongly supported a sister-group relationship between Coleorrhyncha and Auchenorrhyncha (planthoppers, leafhoppers, treehoppers, spittlebugs and cicadas). To test these two alternative hypotheses, we examined the fore- and hindwing base structure of the only known extant macropterous species of Coleorrhyncha using binocular and confocal laser scanning microscopes and analyzed the data selected from the wing base phylogenetically. When full morphological data including the wing base characters were analyzed, the sister group relationship between Coleorrhyncha + Heteroptera was supported, agreeing with previous consensus based on morphology. In contrast, when only wing base characters were analyzed separately, the clade Coleorrhyncha + Auchenorrhyncha was recovered, in agreement with the result from the phylogenomic study. The membranous condition of the proximal median plate in the forewing was identified as a potential synapomorphy of the latter grouping, and absence of the tegula was excluded as a potential synapomorphy of Coleorrhyncha and Heteroptera.

Key words: Auchenorrhyncha – Coleorrhyncha – Heteroptera – phylogeny – wing base structure

Introduction

The suborder Coleorrhyncha (moss bugs) is an enigmatic taxon of the order Hemiptera (Insecta). It consists of a single family, Peloridiidae, with fewer than 40 extant species restricted to circumantarctic regions (Burckhardt 2009; Burckhardt et al. 2011). With a combination of plesiomorphic and apomorphic features, the placement of this suborder within Hemiptera had been highly unstable. Traditionally, prior to explicit phylogenetic analyses of Hemiptera as a whole, Coleorrhyncha was regarded as a member of "Homoptera" (now generally regarded as a paraphyletic grade) due to presence of a complete tentorium, origin of the labium on the posteroventral portion of the head (and absence of a gula), discrete pro- and mesothracic ganglia, and eight pairs of abdominal spiracles, all of which are now regarded as plesiomorphies (Carver et al. 1991). In contrast, Coleorrhyncha share some apparent morphological apomorphies with Heteroptera (reviewed in Grimaldi and Engel 2005; Forero 2008; Burckhardt 2009), some of which have been controversial (e.g., Cobben 1978 but see also Schuh 1979). Recent extensive morphology-based cladistic analysis, with revised morphological observations including Coleorrhyncha, strongly supported Coleorrhyncha + Heteroptera (Friedemann et al. 2014). Multiple molecular phylogenetic studies based on 18S rRNA (Wheeler et al. 1993; Campbell et al. 1995; Ouvrard et al. 2000) and multiple gene regions (Cryan and Urban 2012) also provided support for this relationship. Therefore, until recently, available data appear to have converged toward consensus in support of the sister group relationship between Coleorrhyncha and Heteroptera (together referred to as Heteropterodea or Prosorrhyncha) (Grimaldi and Engel 2005; Forero 2008).

However, a recent phylogenomic study of Hexapoda that incorporated data from >1400 gene regions (Misof et al. 2014) casted doubt on this general view, placing Coleorrhyncha consistently as sister to Auchenorrhyncha (infraorder composed of planthoppers, leafhoppers, treehoppers, spittlebugs and cicadas). This result was supported by multiple datasets (i.e., nucleotide and amino acid sequences) and also received strong statistical support by bootstrapping and four-cluster likelihood mapping analyses (Misof et al. 2014, Supplement). The previously accepted sister group relationship between Coleorrhyncha and Heteroptera was also refuted by recent mitochondrial phylogenomic analyses (Cui et al. 2013; Wang et al. 2015). Therefore, an apparent conflict between morphological and molecular data has arisen in the placement of Coleorrhyncha.

The wing base structure comprises sclerites located between the insect thorax and wing. This structure mediates the power produced by the thoracic indirect flight muscles to the wings and also controls proper flapping and folding of the wings. Therefore, evolution of this structure is strongly constrained and, thus, the wing base sclerites appear to evolve very slowly (Hörnschemeyer 2002). Because of this unique property, the wing base structure has previously been utilized for resolving controversial branches in hemipteroid phylogeny. For example, although the monophyly of Auchenorrhyncha has been questioned based on morphological (Bourgoin 1986ab 1993; Bourgoin and Huang 1990) and molecular criteria (Campbell et al. 1995; Sorensen et al. 1995; Bourgoin et al. 1997; Ouvrard et al. 2000), examination of wing base morphology provided unambiguous support for Auchenorrhyncha (Yoshizawa and Saigusa 2001). Monophyly of Auchenorrhyncha subsequently received strong support from the molecular phylogenetic (Urban and Cryan 2007; Cryan and Urban 2012) and phylogenomic (Misof et al. 2014) analyses, corroborating the value of wing base structure for resolving difficult higher-level phylogenetic problems (see also Yoshizawa 2011).

In this study, we examined the morphology of the fore- and hindwing base structures of a species of Coleorrhyncha, which were treated as missing characters by Friedemann et al. (2014), to test the alternative hypotheses on the phylogenetic placement of this suborder.

Material and Methods

A dried specimen of *Peloridium hammoniorum* Breddin, 1897 collected in Chile in 2014 by CHD was used. This is the only extant species of Coleorrhyncha known to have flight ability, although most individuals of this species have vestigial hindwings. The individual studied possessed fully developed fore- and hindwings. The specimen was soaked with 10% KOH at room temperature for one night. Later, the pterothorax was separated from the other body parts, washed by distilled water, then 80% ethanol, and finally stored and observed in glycerol.

Observations were made with an Olympus SZX 16 binocular microscope (Olympus Co., Tokyo, Japan) and Leica TCS-SP5 Confocal Laser Scanning Microscope (CLSM) (Leica Microsystems, Wetzlar, Germany). For binocular microscope observation, the dissected specimen was pinned on a polyfoam using micro-pins, with the wings fully opened

but oriented in a slight downstroke position to observe all the sclerites in their natural shapes dorsally. For CLSM imaging, specimens were mounted on a large cover glass (22 x 24 mm) covered by a small cover glass (15 mm ø) to facilitate the observation of both dorsal and ventral sides. We used an excitation wavelength of 488 nm and emission wavelength of 510–680 nm. The emission waves were detected using two channels and visualized with two pseudocolors (510–580 nm in green; 580–680 nm in red) (Mikó and Deans 2014). Homology was assessed following Yoshizawa and Saigusa (2001), in which the criteria and landmarks for homology identification of paraneopteran (hemipteroid) wing base sclerites were explained. Terminology of Yoshizawa and Saigusa (2001) was also adopted.

Morphological data selected from the forewing base of *Peloridium* were newly appended to two data matrices created previously: (1) the forewing base character matrix for Paraneoptera, comprising 20 discrete characters, constructed by Yoshizawa and Saigusa (2001), in which Coleorrhyncha was not examined; (2) the full morphological data, comprising 119 characters (including the above as characters 20–39) compiled by Friedemann et al. (2014), with some corrections to character coding as mentioned by Yoshizawa and Lienhard (2016). The genus *Hackeriella* was used in the original full morphological data matrix (Friedemann et al. 2014) but, because this genus lacks flight ability, almost all wing base characters were previously coded as unknown. Here, the same set of wing base characters scored for the separate wing base matrix was newly appended to the matrix. Although this combination of data from two different peloridiid species created a chimeric OTU in the data matrix, members of the family appear to be invariant for most (if not all) of the included characters, so we would not anticipate a different phylogenetic result had we scored all of Friedemann's characters for *Peloridium*. The hindwing base structure was also observed but not included in the phylogenetic analyses to avoid the possibility of over-weighting serially homologous (non-independent) traints, as discussed by Yoshizawa and Saigusa (2001). Data matrices are available as online Supporting Information. The datasets were analyzed by the maximum parsimony method using PAUP* 4a152 (Swofford 2002), with all characters weighted equally and branch-and-bound search performed. The branch-and-bound method uses an exact algorithm that is guaranteed to find the most parsimonious tree(s). Bootstrap and jackknife values were calculated using PAUP* with 1000 replicates (for jackknifing, version 4b10 was used because of problematic values provided by 4a152). For bootstrapping and jackknifing, heuristic searches with

tree-bisection-reconnection algorithm were performed, each with 100 replications and with maxtrees = 10000. The decay index was calculated by using TreeRot V3 (Sorenson and Franzosa 2007). The character state changes were calculated using MacClade 4 (Maddison and Maddison 2001), and unambiguous character state changes were mapped onto the tree.

Results

Forewing base morphology (Fig. 1)

The anterior and median notal wing processes (ANWP and MNWP) are easily identified as articular points with 1Ax: the former is well projecting but the latter is not. The posterior notal wing process (PNWP) is less recognizable because it does not project and is loosely associated with the third axillary sclerite. The tegula (Tg) is apparently present but weakly sclerotized. The humeral plate (HP) is united with the basisubcostale (BSc). The basiradiale (BR) is broadly united with BSc anteriorly, and is united with the second axillary sclerite (2Ax) posteroproximally. The first axillary sclerite (1Ax) is subtriangular in shape (see Fig. 1A; 1Ax is oriented laterally in Fig. 1B), lacking the anterior arm, with a weak swelling on the proximal margin which articulates with MNWP. The anterior tip of 1Ax articulates with the tip of BSc. The posteroproximal margin of 1Ax is also associated with the notum. Distally, 1Ax articulates with 2Ax at two points; near the anterior tip and near the posterodistal corner. 2Ax is subdivided into two sclerites, posteroproximal (pp) and anterodistal (ad), clearly divided by a membranous region and the forked convex axillary fold line. 2Ax-pp is tightly united with the apex of BSc anteroproximally and is articulated with the well-developed and narrowly extended anterior arm of the third axillary sclerite (3Ax) at its distal end. 2Ax-ad is united distally with the first distal median plate, and the convex axillary fold line forms a border between the two sclerites. The proximal arm of 3Ax is broadened and loosely articulated with the notum. Distally, it is tightly associated with the basianal (BA) along the posterior margin (see Fig. 1A,C: in Fig. 1B, 3Ax and BA are detached but this was caused artificially by slide mounting pressure). BA is well developed, tightly articulated with the anal vein distally. The region corresponding to the proxomal median plate (PMP) is completely membranous (see Fig. 1C). The distal median plate (DMP) is subdivided into two elements. DMP1 is enlarged and convex dorsally. It is united proximally with 2Ax, tightly associated with vein R anteriorly, and tightly articulated with

vein A posterodistally. DMP2 is located distal to DMP1, triangular in shape and very narrowly extending toward the claval fold. The jugum (Jg) is apparently not developed.

Hindwing base morphology (Fig. 2)

[Note for CLSM image (Fig. 2B): Due to the less tight articulation of the hindwing sclerites and pressure caused during slide mounting, the positions of many sclerites in the CLSM image are distorted. See the line drawing (Fig. 2A) for their more natural articular condition.]

ANWP and MNWP are recognizable but very loosely articulated with 1Ax, with the former located anterior to the tip of 1Ax. PNWP is well developed and articulated with 3Ax. Tg is absent. HP is united with BSc. BR is only recognizable as a small projection extending from the posterior margin of BSc, and loosely associates with 2Ax at the tip. 1Ax is narrowed over almost its entire length, only weakly broadened medially along the distal margin, with a weakly developed anterior arm. The anterior tip of 1Ax only weakly articulates with the tip of BSc. Distally, 1Ax articulates with 2Ax only at one point. 2Ax is not subdivided as in the forewing but reduced in size and triangular in shape. It tightly articulates with 1Ax only at its anteroproximal corner and also tightly articulates with 3Ax at its posterior tip. 3Ax is well developed, rather loosely articulated with PNWP. Distally, it is tightly associated with the anal vein (distal margin) and DMP (anterodistal corner). BA is indistinguishable from 3Ax. The region corresponding to PMP is completely membranous. DMP is flat, trapezoidal in shape. Jg is large but only weakly sclerotized.

Phylogenetic analyses

The parsimony analysis of the forewing base dataset resulted in only one most parsimonious tree (Fig. 3: treelength = 23; consistency index = 0.91; retention index = 0.93). This tree is completely congruent with that estimated by Yoshizawa and Saigusa (2001), with monophyly of Paraneoptera, Condylognatha, and Hemiptera all supported. Coleorrhyncha (excluded from the analysis of Yoshizawa and Saigusa 2001) formed a clade together with the auchenorrhynchous infraorders (Cicadomorpha and Fulgoromorpha), supported by one unique, non-homoplasious synapomorphy (decay index = 1): the membranous proximal median plate (Character 13:1).

The parsimony analysis of the full morphology dataset, including the forewing base

characters, resulted in 18 equally parsimonious trees (treelength = 197; consistency index = 0.69; retention index = 0.85). Fig. 4 shows the strict consensus of 18 trees (differences between them mostly concern the arrangements of zero-length branches and do not affect to the following discussion: see Supporting Information for all trees). The tree is congruent with that estimated by Friedemann et al. (2014), with Paraneoptera, Psocodea, Condylognatha, Hemiptera, Auchenorrhyncha and Heteroptera supported as monophyletic. Coleorrhyncha was placed as sister of Heteroptera, with three apomorphies (including two non-homoplasious ones) supporting this placement. One of the characters selected from the wing base (Character 28:1) provided non-homoplasious support for Hemiptera. The character providing support for Auchenorrhyncha + Coleorrhyncha in the wing base dataset (Character 13:1 in the wing base matrix; 32:1 in the full data matrix) was only ambiguously reconstructed: i.e., either independently evolved between Auchenorrhyncha and Coleorrhyncha or gained in the common ancestor of Auchenorrhyncha + Coleorrhyncha + Heteroptera but reversed in Heteroptera.

Discussion

The wing base structure in Coleorrhyncha largely retains the groundplan condition of the neopteran wing base, except for the absence of a proximal median plate (Figs 1–2). All modifications detected previously and thought to be autapomorphic for Hemiptera in general (Yoshizawa and Saigusa 2001) were also observed in Coleorrhyncha. Overall, the wing base structure of Coleorrhyncha resembles that of Auchenorrhyncha rather than Heteroptera (Yoshizawa and Saigusa 2001; Yoshizawa and Wagatsuma 2012; Ogawa et al. 2015). Maximum parsimony analysis of the wing base characters alone clearly supported the monophyly of Coleorrhyncha + Auchenorrhyncha, with absence of PMP as a synapomorphy (Fig. 3: decay index = 1, bootstrap/jackknife values = 67/51%). As mentioned by Yoshizawa and Saigusa (2001), this is a "reduction" character, i.e., presumably resulting from the loss of a sclerite, which may be regarded as less reliable than a character "gain". However, this character state was previously regarded as an autapomorphy of Auchenorrhyncha, a group once thought to be paraphyletic based on early single-gene molecular phylogenies (e.g., Campbell et al. 1995) but more recently supported as monophyletic by multi-gene molecular phylogenies (Urban and Cryan 2007; Cryan and Urban 2012; Misof et al. 2014). In addition,

the present examination clearly identified the tegula on the forewing of Coleorrhyncha, which invalidates ”absence of tegula” as one of the previously proposed synapomorphies of Coleorrhyncha + Heteroptera (Friedemann et al. 2014).

Nevertheless, analysis of the full morphological data still recovered the sister group relationship between the Coleorrhyncha and Heteroptera (Fig 4: Friedemann et al. 2014), although with lower support values (decay index = 1, bootstrap/jackknife values = 52/47%). Synapomorphies supporting this relationship include presence of cephalic trichobothria (54-1), tubular and four-segmented labium (56-2), and four-segmented flagellomeres (59-1). The first two are non-homoplasious characters (Friedemann et al. 2014) in the present dataset. The full morphological matrix constructed by Friedemann et al. (2014) lacked some morphological characters previously suggested as additional synapomorphies of Coleorrhyncha + Heteroptera (Grimaldi and Engel 2005; Forero 2008; Burckhardt 2009; Spangenberg et al. 2013) so it is possible that morphological support for the monophyly of this group is stronger than shown in our analysis.

In contrast, morphological support for the Coleorrhyncha + Heteroptera may not be as robust as generally assumed. For example, the position of abdominal spiracle 2 on an epipleurite was previously suggested as a potential synapomorphy of Coleorrhyncha and Auchenorrhyncha (Sweet 1996). However, because almost all other morphological characters supported a closer relationship between Coleorrhyncha and Heteroptera, Sweet (1996) concluded that the spiracle condition was independently gained by Coleorrhyncha and Auchenorrhyncha. The cephalic trichobothria (54-1) were scored as present for Coleorrhyncha and Heteroptera (Friedmann et al. 2014) and identified as one of their non-homoplasious synapomorphies (Fig. 3). However, the cephalic trichobothria were not illustrated or reported in the recent detailed study of the adult head of *Hackeriella* (Spangenberg et al. 2013) so the status of this character as a synapomorphy of Coleorrhyncha + Heteroptera is questionable. Spangenberg et al. (2013) further reviewed morphological evidence supporting the monophyly of Coleorrhyncha + Heteroptera but pointed out that the homologies of some potential synapomorphies (e.g., the number of antennomeres) remain uncertain while others (e.g., absence of cervical sclerites) are homoplasious. They also noted several potential synapomorphies of Coleorrhyncha and Auchenorrhyncha, or Coleorrhyncha and "Homoptera" in general. Some of the latter, including absence of a gula and presence of a complete tentorium, were interpreted as plesiomorphic for Hemiptera as a whole, but

presence of Evans' organ (Bourgoin 1986b) may be another unique synapomorphy of Coleorrhyncha and Auchenorrhyncha or an autapomorphy of "Homoptera" (including Coleorrhyncha). Characters of the cephalic musculature were found that support either Coleorrhyncha + Heteroptera or Coleorrhyncha + "Homoptera" (Spangenberg et al. 2013).

The results from recent phylogenomic analyses (Misof et al. 2014) and the present wing base examination suggest that some of the above-mentioned morphological similarities between Coleorrhyncha and Auchenorrhycha may be their true synapomorphies. In addition, some of the features previously interpreted as synapomorphies of Coleorrhyncha and Heteroptera (Schlee 1969) have already been considered as "superficial and probably not significant" (Cobben 1978: but see also Schuh 1979 for critique). Based on our study, we also exclude "absence of the tegula" (20-1) as a synapomorphy of Coleorrhyncha + Heteroptera. This resulted in a decrease in branch support for this clade from decay index of three (Friedemann et al. 2014) to only one (Fig. 4). Further morphological investigations, including re-evaluation of the previously proposed synapomorphies of Coleorrhyncha and Heteroptera and incorporation of these and various cephalic characters mentioned by Spangenberg et al. (2013) into an explicit phylogenetic analysis, are needed to elucidate the extent of conflict between morphology and phylogenomics and between different morphological character systems.

Acknowledgments

This study was partly supported by Japan Society for the Promotion of Science pre-doctoral fellowship program (15J03697) to NO and U.S. National Science Foundation grant DEB-1239788 to CHD.

References

Bourgoin T (1986a) Morphologie imaginale du tentorium des Hemiptera Fulgoromorpha. Int J Ins Morph Embryo **15**:237–252.

Bourgoin T (1986b) Valeur morphologique de la lame maxillaire chez les Hemiptera; remarques phylogénétiques. Ann Soc Entomol France (NS) **22**:413–422.

Bourgoin T (1993) Female genitalia in Hemiptera Fulgoromorpha, morphological and phylogenetic data. Ann Soc Entomol France (NS) **29**:225–244.

290 Bourgoin T, Huang J (1990) Morphologie comparée des genitalia mâles des
291 Trypertimorphini et remarques phylogénétiques (Hemiptera: Fulgoromoprha:
292 Tropiduchidae). Ann Soc Entomol France (NS) **26**:555–564.
293 Bourgoin T, Steffen-Campbell JD, Campbell BC (1997) Molecular phylogeny of
294 Fulgoromorpha (Insecta, Hemiptera, Archaeorrhyncha). The Enigmatic
295 Tettigometridae: Evolutionary Affiliations and Historical Biogeography. Cladistics
296 **13**:207–224.
297 Breddin G (1897) Hemipteren (Hemiptera). Ergebnisse der Hamburger magalhaensischen
298 Sammelreise, 1892/93, vol. 2. L. Friederichsen and Co., Humburg.
299 Burckhardt D (2009) Taxonomy and phylogeny of the Gondowanan moss bugs or
300 Peloridiidae (Hemiptera, Coleorrhyncha). Dtsch Entomol Ztg **56**:173–235.
301 Burckhardt D, Bochud E, Damgaard J, Bibbs GW, Hartung V, Larivière MC, Wyniger D,
302 Zürcher I (2011) A review of the moss bug genus *Xenophyes* (Hemiptera:
303 Coleorrhyncha: Peloridiidae) from New Zealand: systematics and biogeography.
304 Zootaxa **2923**:1–26.
305 Campbell BC, Steffen-Campbell JD, Sorensen JT, Gill RJ (1995) Paraphyly of Homoptera
306 and Auchenorrhyncha inferred from 18S rDNA nucleotide sequences. Syst Entomol
307 **20**:175–194.
308 Carver M, Gross GG, Woodward TE (1991) Hemiptera (Bugs, leafhoppers, cicadas, aphids,
309 scale insects etc). In: CSIRO (ed), The Insects of Australia. 2nd edition. Cornell
310 University Press, New York, pp 429–509.
311 Cobben RH (1978) Evolutionary trends in Heteroptera Part II. Mouthpart-structures and
312 feeding strategies. Mededelingen Landbouwhogeschool Wageningen **78**(5):1–407.
313 Cryan JR, Urban JM (2012) Higher-level phylogeny of the insect order Hemiptera: is
314 Auchenorrhyncha really paraphyletic? Syst Entomol **37**:7–21.
315 Cui Y, Xie Q, Hua J, Dang K, Zou J, Liu X, Wang G, Yu X, Bu W (2013) Phylogenomics of
316 Hemiptera (Insecta: Paraneoptera) based on mitochondrial genomes. Syst Entomol
317 **38**:233–245.
318 Forero D (2008) The systematics of the Hemiptera. Rev Columbiana Entomol **34**:1–21.
319 Friedemann K, Spangenberg R, Yoshizawa K, Beutel RG (2014) Evolution of attachment
320 structure in the highly diverse Acercaria (Hexapoda). Cladistics **30**:170–201.
321 Grimaldi D, Engel MS (2005) Evolution of the Insects. Cambridge Univ. Press, Cambridge.

322 Hörnschemeyer T (2002) Phylogenetic significance of the wing-base of the Holometabola
323 (Insecta). Zool Scripta **31**:17–29.
324 Maddison DR, Maddison WP (2001) MacClade 4: Analysis of Phylogeny and Character
325 Evolution. Sinauer Inc., Sunderland.
326 Mikó I, Deans AR (2014) The second axillary in Hymenoptera. PeerJ PrePrints **2**:e428v1.
327 http://dx.doi.org/10.7287/peerj.preprints.428v1
328 Misof B, Liu S, Meusemann K et al. (2014) Phylogenomics resolves the timing and pattern of
329 insect evolution. Science **346**:763–767.
330 Ogawa N, Maruyama M, Yoshizawa K (2015) Wing base morphology of Aetalionidae
331 (Hemiptera: Cicadomorpha) and its phylogenetic implications. Entomol Sci **18**:262–
332 265.
333 Ouvrard D, Campbell BC, Bourgoin T, Chan KL (2000)18S rRNA secondary structure and
334 phylogenetic position of Peloridiidae (Insecta, Hemiptera). Mol Phylog Evol **16**:403–
335 417.
336 Schlee D (1969) Hennig's principles of phylogenetic systematics, and 'intuitive
337 statisticophenetic taxonomy'? A reply to Dr. Coless' paper 'The phylogenetic fallacy'.
338 Syst Zool **18**:127–134.
339 Schuh RT (1979) Review: Evolutionary Trends in Heteroptera. Part II. Mouthpart-Structure
340 and Feeding Strategies. By R. H. Cobben. Syst Zool **28**:653–656.
341 Sorensen JT, Campbell BC, Gill RJ, Steffen-Campbell JD (1995) Non-monophyly of
342 Auchenorrhyncha ("Homoptera"), based upon 18S rDNA phylogeny: Eco-evolutionary
343 and cladistic implications within pre-Heteropterodea Hemiptera (s.l.) and a proposal for
344 new monophyletic suborders. Pan-Pacific Entomol **71**:31–60.
345 Sorenson MD, Franzosa EA (2007) TreeRot, Version 3. Boston Univ., MA.
346 Spangenberg R, Wipfler B, Friedemann K, Pohl H, Weirauch C, Hartung V, Beutel RG
347 (2013) The cephalic morphology of the Gondwanan key taxon *Hackeriella*
348 (Coleorrhyncha, Hemiptera). Arthropod Struct Dev **42**:315-337.
349 Sweet MH (1996) Comparative external morphology of the pregenital abdomen of the
350 Hemiptera. In: Schaefer, C.W. (ed), Studies on Hemipteran Phylogeny, Entomological
351 Society of America, Maryland, pp 119–158.
352 Swofford DL (2002) PAUP*: Phylogenetic Analysis Using Parsimony (* and Other
353 Methods), Version 4. Sinauer Inc., Sunderland.

354 Urban JM, Cryan JR (2007) Evolution of the planthoppers (Insecta: Hemiptera: Fulgoroidea).
355 Mol Phylog Evol **42**:556–572.
356 Wang Y, Chen J, Jiang LY, Qiao GX (2015) Hemipteran mitochondrial genomes: Features,
357 structures and implications for phylogeny. Int J Mol Sci **16**:12382–12404.
358 Wheeler WC, Schuh RT, Bang R (1993) Cladistic congruence among higher groups of
359 Heteroptera: congruence between morphological and molecular data sets. Entomol
360 Scandinavica **42**:121–137.
361 Yoshizawa K (2011) Monophyletic Polyneoptera recovered by wing base structure. Syst
362 Entomol **36**:377–394.
363 Yoshizawa K, Lienhard C (2016) Bridging the gap between chewing and sucking in the
364 hemipteroid insects: new insights from Cretaceous amber. Zootaxa **4079**:229–245.
365 Yoshizawa K, Saigusa T (2001) Phylogenetic analysis of paraneopteran orders (Insecta:
366 Neoptera) based on forewing base structure, with comments on monophyly of
367 Auchenorrhyncha (Hemiptera). Syst Entomol **26**:1–13.
368 Yoshizawa K, Wagatsuma M (2012) Phylogenetic relationships among superfamilies of
369 Cicadomorpha (Hemiptera: Auchenorrhyncha) inferred from the wing base structure.
370 Entomol Sci **15**:408–421.
371
372

Figure caption

Fig. 1. Forewing base structure of Coleorrhyncha. A. Line drawing, dorsal view. B. Image taken by CLSM, dorsal view. The base of the anal vein is strongly expanded and covers most of the membranous PMP (see also C). Note: the detachment between 3Ax and BA is an artifact caused by slide-mounting pressure (see A and C for their natural relationship). C. Ventral view of wing base, showing PMP region and surrounding structures. The structure in the background of the completely membranous PMP is the expanded base of the anal vein (see B for comparison).

Fig. 2. Hindwing base structure of Coleorrhyncha. A. Line drawing, dorsal view. B. Image taken by CLSM, dorsal view. Note: distortion in relative position of the notum and axillary sclerites are an artifact caused by slide-mounting pressure (see A for their natural relationship).

Fig. 3. The most parsimonious tree estimated from the wing base data (outgroups are omitted), with characters and their changes noted on the branched. A red square indicates a non-homoplasious change, and a gray triangle indicates a homoplasious change. Circled numbers are decay indices, and numbers in a square indicate bootstrap/jackknife values of adjacent branches.

Fig. 4. The strict consensus of 18 equally parsimonious trees estimated from the full morphological data set. See Fig. 3 for further explanations. Polytomies were treated as hard polytomy for character state reconstruction. Outgroups are omitted from the figure.

Appendix: Characters and their state used for phylogenetic analyses.

Forewing base data (modified from Yoshizawa and Saigusa 2001)

1. Tg: (0) present; (1) absent: ci = 1, ri = 1.
2. Tg: (0) small; (1) enlarged, with broad extention encircling the entire margin: ci = 1, ri = 0.
3. Tg: (0) with small attachment to body wall; (1) with broad attachment to body wall: ci = 1, ri = 0.
4. HP and BSc: (0) separate from each other; (1) united with each other: ci = 1, ri = 1.
5. BSc: (0) distant from 2Ax; (1) close proximity to anteroproximal corner of 2Ax; (2) fused with anteroproximal part of 2Ax: ci = 1, ri = 1.
6. BR and HP + BSc: (0) fused with each other; (1) separated from each other: ci = 1, ri = 0.
7. BR and 2Ax: (0) separate from each other; (1) fused: ci = 0.5, ri = 0.
8. 2Ax: (0) nearly flat; (1) anterior region swollen: ci = 1, ri = 1.
9. 2Ax: (0) not divided; (1) divided into two sclerites (2Ax-pp and -ad): ci = 1, ri = 1.
10. PMP: (0) located distal to 2Ax; (1) located posterodistally to 2Ax: ci = 1, ri = 1.
11. PMP: (0) nearly flat; (1) deeply concave: ci = 1, ri = 1.
12. PMP: (0) almost evenly sclerotized; (1) distal margin sclerotized more strongly than its other regions: ci = 1, ri = 1.
13. PMP: (0) well sclerotized; (1) reduced, often completely membranous: ci = 1, ri = 1.
14. DMP: (0) not divided; (1) divided into 2 sclerites: ci = 1, ri = 1.
15. DMP: (0) distant from 2Ax; (1) placed next to 2Ax, articulating along a convex hinge: ci = 1, ri = 1.
16. DMP: (0) large; (1) reduced in size: ci = 1, ri = 0.
17. Distal arm of 3Ax and DMP: (0) articulate with each other; (1) not articulate with each other: ci = 1, ri = 1.
18. Anterior arm of 3Ax: (0) present; (1) absent: ci = 0.5, ri = 0.
19. 3Ax and BA: (0) separate from posterior margin of forewing base; (1) situated on posterior margin of forewing base: ci = 1, ri = 0.
20. BA and PMP: (0) separate from each other; (1) fused with each other: ci = 1, ri = 1.

Full morphology data (modified from Friedmann et al. 2014)

1. Rupturing mechanism at the base of the antennal flagellum: (0) absent; (1) present: ci = 1,

ri = 1.

2. Exposure of mouthparts: (0) largely or completely exposed; (1) left mandible enclosed in a pouch formed by anteclypeal wall, labrum, stipes, and hypopharynx; (2) bases of mandibular and maxillary stylets articulate inside head with mandibular and maxillary plates: ci = 1, ri = 1.

3. Right mandible: (0) present; (1) reduced: ci = 1, ri = 0.

4. Shape of mandibles: (0) not elongated; (1) elongated: ci = 0.5, ri = 0.92.

5. Cardo: (0) present; (1) strongly reduced or absent; (2) fused with stipes: ci = 1, ri = 1.

6. Lacinia: (0) absent; (1) present: ci = 1, ri = 1.

7. Insertion of lacinia: (0) on stipes; (1) detached from stipes: ci = 0.5, ri = 0.86.

8. Lacinia: (0) not elongate and stylet-like; (1) elongate and stylet-like: ci = 1, ri = 1.

9. Labial rostrum: (0) absent; (1) present: ci = 1, ri = 1.

10. Labial palps: (0) absent or strongly reduced; (1) comprising at least 2 segments: ci = 0.5, ri = 0.86.

11. Cibarial water-vapour uptake apparatus: (0) absent; (1) present: ci = 0.5, ri = 0.80.

12. Jugal “bar”: (0) absent; (1) present: ci = 1, ri = 1.

13. Abdominal ganglia: (0) more than two separate ganglia; (1) two separate ganglia; (2) one single ganglionic mass: ci = 1, ri = 1.

14. Eyes of immature stages: (0) persist; (1) disintegrate or pulled back proximally into cerebrum: ci = 1, ri = 1.

15. External wing buds: (0) present; (1) absent: ci = 1, ri = 1.

16. Pupal stage: (0) absent; (2) present: ci = 0.5, ri = 0.5.

17. Appearance of compound eyes: (0) before ultimate immature stage; (1) in ultimate immature stage: ci = 1, ri = 1.

18. Ocelli of immature stages: (0) present; (1) absent: ci = 1, ri = 1.

19. Cerci of immature stages: (0) present; (1) absent: ci = 1, ri = 1.

20. Tegulae of the forewing: (0) present; (1) absent: ci = 1, ri = 1.

21. Size and shape of tegulae: (0) small; (1) enlarged, with broad extension encircling the entire margin: ci = 1, ri = 1.

22. Attachment of tegulae to body wall: (0) narrow; (1) broad: ci = 0.5, ri = 0.

23. HP and BSc: (0) separated from each other; (1) connected with each other: ci = 1, ri = 0.

24. BSc: (0) distant from 2Ax; (1) closely adjacent with the anteroproximal corner of 2Ax;

(2) fused with anteroproximal part of 2Ax: ci = 0.67, ri = 0.67.

25. BR and HP + BSc: (0) fused with each other; (1) separated from each other: ci = 1, ri = 0.

26. BR and 2Ax: (0) separated from each other; (1) fused: ci = 0.5, ri = 0.

27. 2Ax: (0) nearly flat; (1) anterior region inflated: ci = 1, ri = 1.

28. 2Ax: (0) not divided; (1) not divided: ci = 1, ri = 1.

29. Position of PMP: (0) distad 2Ax; (1) posterodistad 2Ax: ci = 1, ri = 0.

30. PMP: (0) nearly flat; (1) deeply concave: ci = 1, ri = 0.

31. PMP: (0) almost evenly sclerotized; (1) distal margin sclerotized more strongly than its other regions: ci = 1, ri = 0.

32. PMP: (0) well sclerotized; (1) reduced, often completely membranous: ci = 0.5, ri = 0.86.

33. DMP: (0) not divided; (1) divided into 2 sclerites: ci = 1, ri = 0.

34. DMP: (0) distant from 2Ax; (1) placed next to 2Ax, articulating along a convex hinge: ci = 1, ri = 1.

35. DMP: (0) large; (1) reduced in size: ci = 1, ri = 0.

36. Distal arm of 3Ax and DMP: (0) articulating with each other; (1) not articulating with each other: ci = 1, ri = 0.

37. Anterior arm of 3Ax: (0) present; (1) absent: ci = 0.5, ri = 0.

38. 3Ax and BA: (0) separate from posterior margin of forewing base; (1) attached to posterior margin of forewing base: ci = 1, ri = 0.

39. BA and PMP: (0) separate from each other; (1) fused with each other: ci = 1, ri = 0.

40. Lateral hypopharyngeal arm (0) present; (1) absent: ci = 0.5, ri = 0.88.

41. Ovarioles: (0) not polytrophic; (1) polytrophic; (2) telotrophic; (3) panoistic: ci = 0.75, ri = 0.92.

42. Maxillary palps: (0) present, with four segments or more; (1) absent or reduced number of segments: ci = 0.33, ri = 0.8.

43. Abdominal sternite 1: (0) present; (1) absent: ci = 0.5, ri = 0.8.

44. Number of axonemes in spermatozoans: (0) zero; (1) one; (2) two; (3) three: ci = 0.75, ri = 0.83.

45. Gonangulum: (0) not fused with tergum IX; (1) fused with tergum IX: ci = 0.5, ri = 0.8.

46. Pretentorium: (0) absent or if present not connecting internal extremities of mandibular lever and corpotentorium; (1) unites internal extremities of mandibular lever and corpotentorium: ci = 1, ri = 1.

47. Lacinial gland: (0) absent; (1) present: ci = 0.5, ri = 0.

48. Male genitalia: (0) symmetrical, or if asymmetrical, asymmetry not involving pregenital segments; (1) asymmetrical, this asymmetry often involving pregenital segments: ci = 0.5, ri = 0.

49. Accessory salivary glands generally: (0) not tubular; (1) of the tubular type: ci = 1, ri = 0.

50. Number of eye trichobothria of first instars: (0) one or absent; (1) two: ci = 1, ri = 0.

51. Number of ommatidia in first-instar larvae: (0) 4-5; (1) more than five: ci = 0.5, ri = 0.

52. Number of tarsomeres in first-instar larvae: (0) one; (1) two: ci = 1, ri = 1.

53. Forewings: (0) completely uniform or if differentiated, not forming a distinct corium-clavus and membrane; (1) forewing divided into a distinct corium-clavus and membrane: ci = 0.5, ri = 0.

54. Cephalic trichobothria: (0) absent in adults; (1) present in adults: ci = 1, ri = 1.

55. Metathoracic scent gland system: (0) absent; (1) present: ci = 1, ri = 1.

56. Labium: (0) not tubular; (1) tubular labium with three segments; (2) tubular labium with four segments: ci = 1, ri = 1.

57. Insertion of tubular labium: (0) posteriorly on the head, (1) anteriorly on the head: ci = 1, ri = 1.

58. Dorsal abdominal glands in immature stages: (0) absent; (1) present: ci = 1, ri = 1.

59. Number of antennal flagellomeres: (0) more than 4, (1) 4 or less: ci = 0.33, ri = 0.75.

60. Articulations between the mesomere, anterodorsal extension of ventral plate and posterior end of basal plate: (0) absent; (1) present: ci = 0.5, ri = 0.5.

61. Length of basal apodeme of the phallic organ: (0) short; (1) long, longer than basal plate: ci = 1, ri = 0.

62. Third posterodorsal corner of basal plate: (0) not extended; (1) extended posteriorly: ci = 1, ri = 0.

63. Basal apodeme of the phallic organ: (0) present; (1) absent: ci = 1, ri = 1.

64. Width of basal apodeme: (0) narrow; (1) as broad as or broader than basal plate: ci = 1, ri = 1.

65. Ventral plates 1: (0) separated; (1) partly fused anteriorly: ci = 1, ri = 1.

66. Ventral plates 2: (0) separated or partly fused; (1) completely fused: ci = 1, ri = 0.

67. Mesomere of the aedeagus: (0) rounded posteriorly; (1) pointed posteriorly: ci = 0.5, ri = 0.5.

68. Posteromedian part of basal plate: (0) membranous; (1) sclerotized: ci = 1, ri = 1.

69. Anterior end of mesomere: (0) articulated with basal plate; (1) articulated with paramere: ci = 1, ri = 0.

70. Paired ocelli in nymphs or larvae: (0) absent; (1) present: ci = 1, ri = 1.

71. Intrinsic antennal muscles (Mm. scapopedicellares) in immature stages: (0) absent; (1) present: ci = 1, ri = 1.

72. Ventral metasternal process: (0) absent; (1) present: ci = 1, ri = 1.

73. Sensory plate organs of pedicel: (0) absent; (1) present: ci = 1, ri = 1.

74. Evan's organ: (0) absent, (1) present: ci = 0.5, ri = 0.86.

75. Ductus ejaculatorius: (0) normal; (1) modified as a sperm pump: ci = 1, ri = 1.

76. Proximal abdomen pediculate by reduction of the 1st and 2nd segment: (0) absent; (1) present: ci = 1, ri = 1.

77. Hind coxae: (0) normally developed; (1) broad, closely adjacent: ci = 1, ri = 1.

78. Proboscis: (0) absent; (1) shifted posteriorly between bases of procoxae; (2) not shifted posteriorly between bases of procoxae: ci = 0.67, ri = 0.94.

79. Posterior parts of the head capsule: (0) sclerotized; (1) membraneous: ci = 1, ri = 1.

80. Connective tissue occluding occipital foramen: (0) absent; (1) present: ci = 0.5, ri = 0.

81. Ovipositor simplified: (0) absent; (1) present: ci = 0.5, ri = 0.5.

82. Spiracular glands: (0) absent; (1) present: ci = 0.5, ri = 0.

83. Extension of the occipital apodeme reaching into the thorax: (0) absent; (1) present: ci = 0.5, ri = 0.

84. Pronotum and procoxae: (0) not fused; (1) fused: ci = 1, ri = 1.

85. Position of anterior tentorial pits: (0) frontal side of head; (1) absent; (2) shifted dorsally: ci = 1, ri = 1.

86. Fusion of head and thorax: (0) absent; (1) present: ci = 1, ri = 1.

87. Body and head: (0) not flattened; (1) dorsoventrally flattened: ci = 0.25, ri = 0.67.

88. Hind femora: (0) not enlarged; (1) enlarged: ci = 0.33, ri = 0.6.

89. Meso- and metanotum: (0) not fused; (1) fused: ci = 1, ri = 1.

90. Compound eyes: (0) not reduced; (1) only 2 ommatidia or less: ci = 0.5, ri = 0.86.

91. Labial palp: (0) present; (1) absent: ci = 0.5, ri = 0.88.

92. Complex tymbal acoustic system: absent (0); present (1): ci = 1, ri = 1.

93. Aristate antennal flagellum: (0) absent; (1) present: ci = 0.5, ri = 0.86.

94. Malpighian tubules: (0) more than six; (1) six; (2) four or less: ci = 1, ri = 1.

95. Labrum: (0) not narrowed; (1) narrowed: ci = 1, ri = 1.

96. Mandibular and lacinial stylets: (1) unicondylar; (0) dicondylar: ci = 1, ri = 1.

97. Pedunculate eggs (with stalk): (0) absent; (1) present: ci = 1, ri = 1.

98. Gut with filter chamber containing Malpighian tubules: (0) absent; (1) present: ci = 1, ri = 1.

99. Coronal (= median epicranial) suture: (0) absent; (1) present: ci = 0.33, ri = 0.33.

100. Parempodia on unguitractor plate: (0) absent; (1) elongate and setiform, inserted in an alveolus: ci = 0.5, ri = 0.5.

101. Number of tarsal segments: (0) one; (1) two; (2) three; (3) more than three. State 3 is adopted for Mydiognathus: ci = 0.33, ri = 0.65.

102. Arolium: (0) absent; (1) present; (2) eversible; (3) bilobed: ci = 0.33, ri = 0.45.

103. Sticky terminal lip of arolium: (0) absent; (1) present: ci = 0.5, ri = 0.67.

104. Pulvilli: (0) absent; (1) present: ci = 0.33, ri = 0.6.

105. Euplantulae: (0) absent, (1) present: ci = 0.33, ri = 0.33.

106. Number of claws: (0) one; (1) two; (2) reduced into spoon-shaped plates; (3) main claw plus accessory claw: ci = 0.75, ri = 0.67.

107. Claw teeth: (0) absent; (1) present: ci = 0.33, ri = 0.33.

108. Protuberance with microtrichia on distolateral side of the pretarsus: (0) absent; (1) present: ci = 1, ri = 0.

109. Sensorial setae on mesal side of arolium: (0) absent; (1) present: ci = 1, ri = 1.

110. Adhesive claw setae: (0) absent; (1) present: ci = 1, ri = 0.

111. Eversible structure between tibia and tarsus: (0) absent; (1) present: ci = 0, ri = 0.

112. Tibial thumb-like process: (0) absent; (1) present: ci = 1, ri = 0.

113. Empodial paronychium: (0) absent; (1) present: ci = 1, ri = 0.

114. Tarsal apophysis on the ventral side of the tarsus: (0) absent; (1) present: ci = 1, ri = 0.

115. Two dorsal capitate setae: (0) absent; (1) present: ci = 1, ri = 0.

116. Flag-like sensilla on the 1st tarsal segment: (0) absent; (1) present: ci = 1, ri = 0.

117. Fingerlike process below claw: (0) absent; (1) present: ci = 1, ri = 0.

118. Ventral brush: (0) absent; (1) present: ci = 0.5, ri = 0.

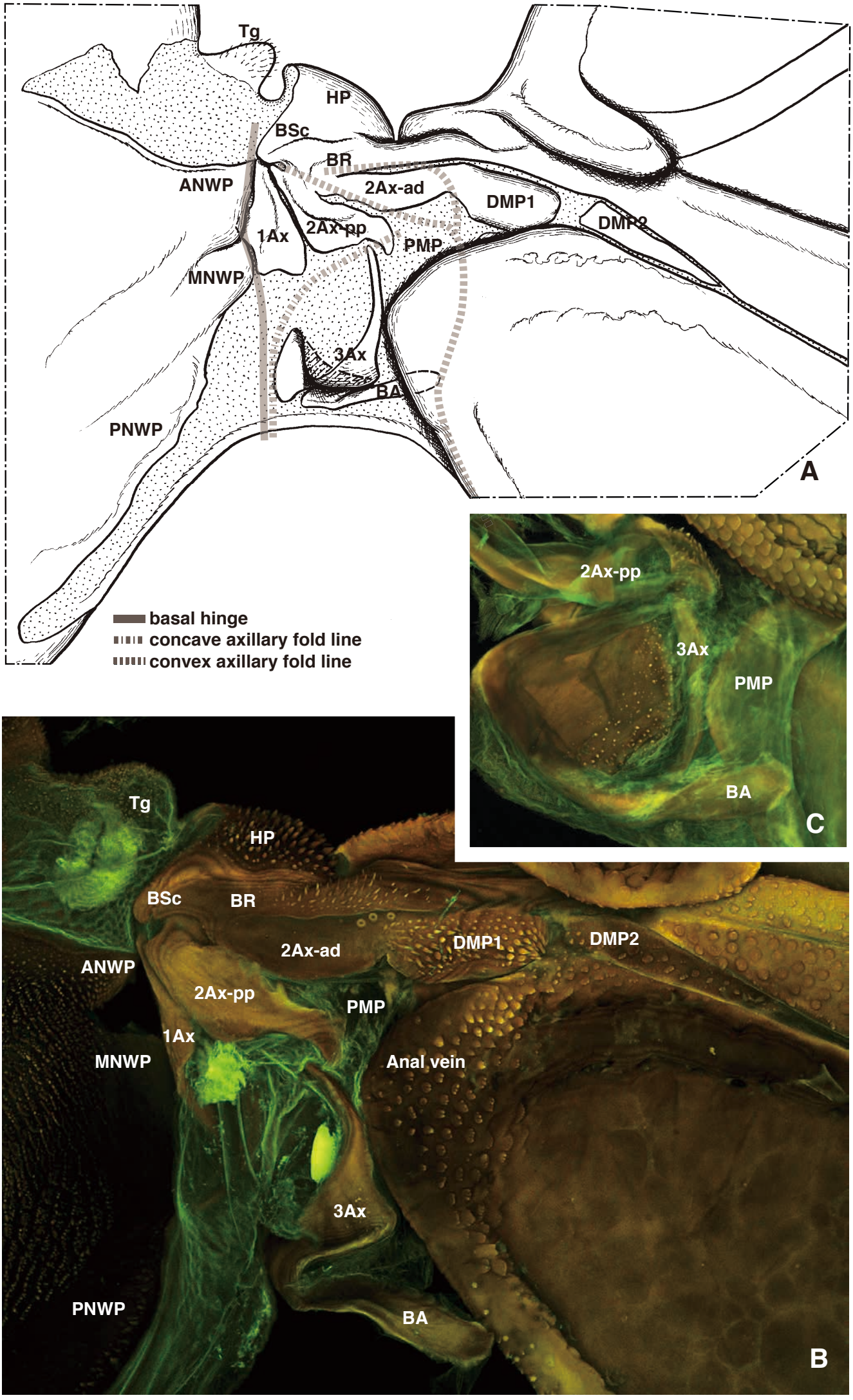
Tg
HP
BSc
BR
ANWP
2Ax-ad
DMP1
DMP2
1Ax
2Ax-pp
PMP
MNWP
3Ax
BA
PNWP
A
basal hinge
concave axillary fold line
convex axillary fold line
2Ax-pp
3Ax
PMP
BA
C
Tg
HP
BSc
BR
2Ax-ad
DMP1
DMP2
ANWP
2Ax-pp
PMP
1Ax
MNWP
Anal vein
3Ax
PNWP
BA
B

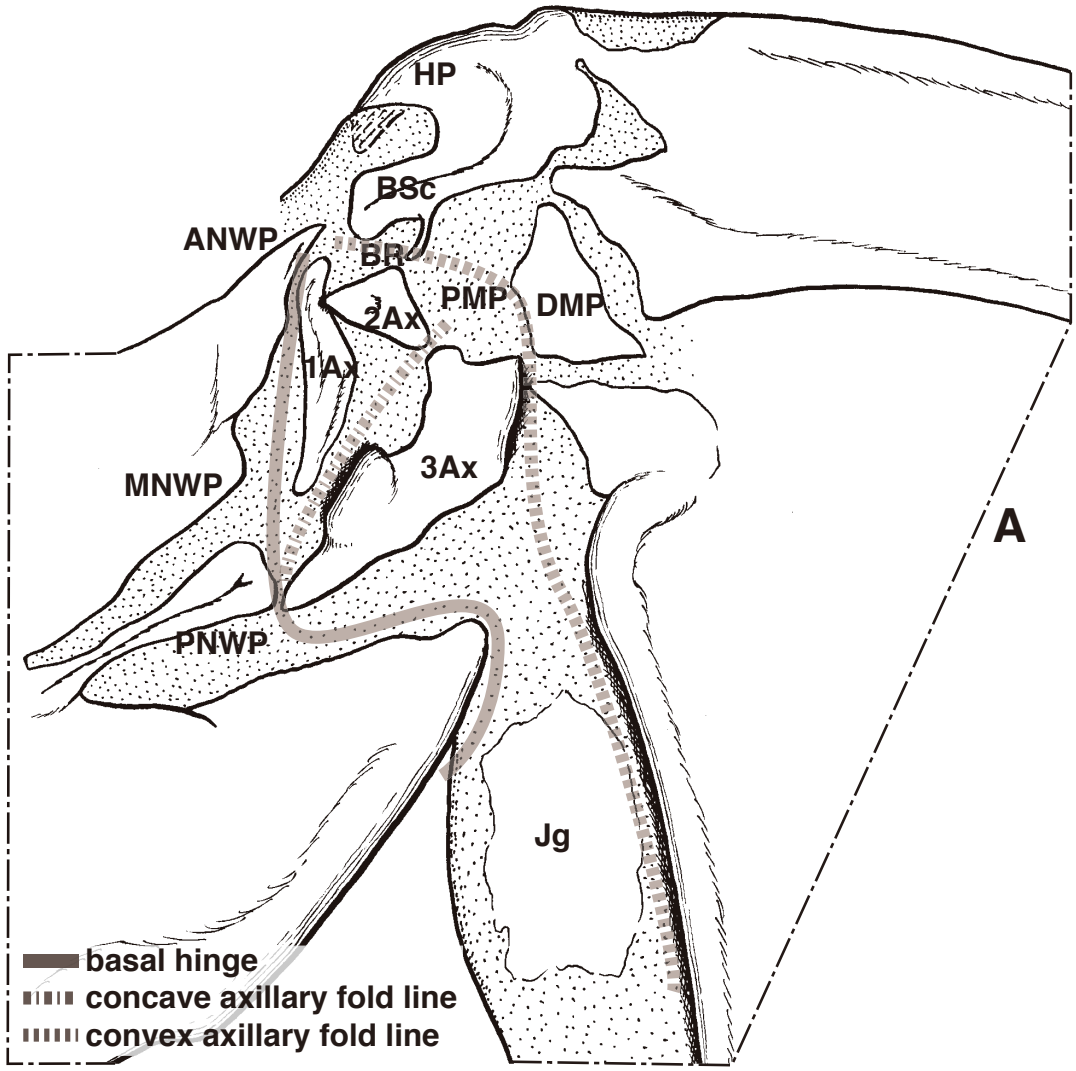
HP
BSc
ANWP
BR
PMP
DMP
2Ax
1Ax
3Ax
MNWP
PNWP
Jg
A
basal hinge
concave axillary fold line
convex axillary fold line

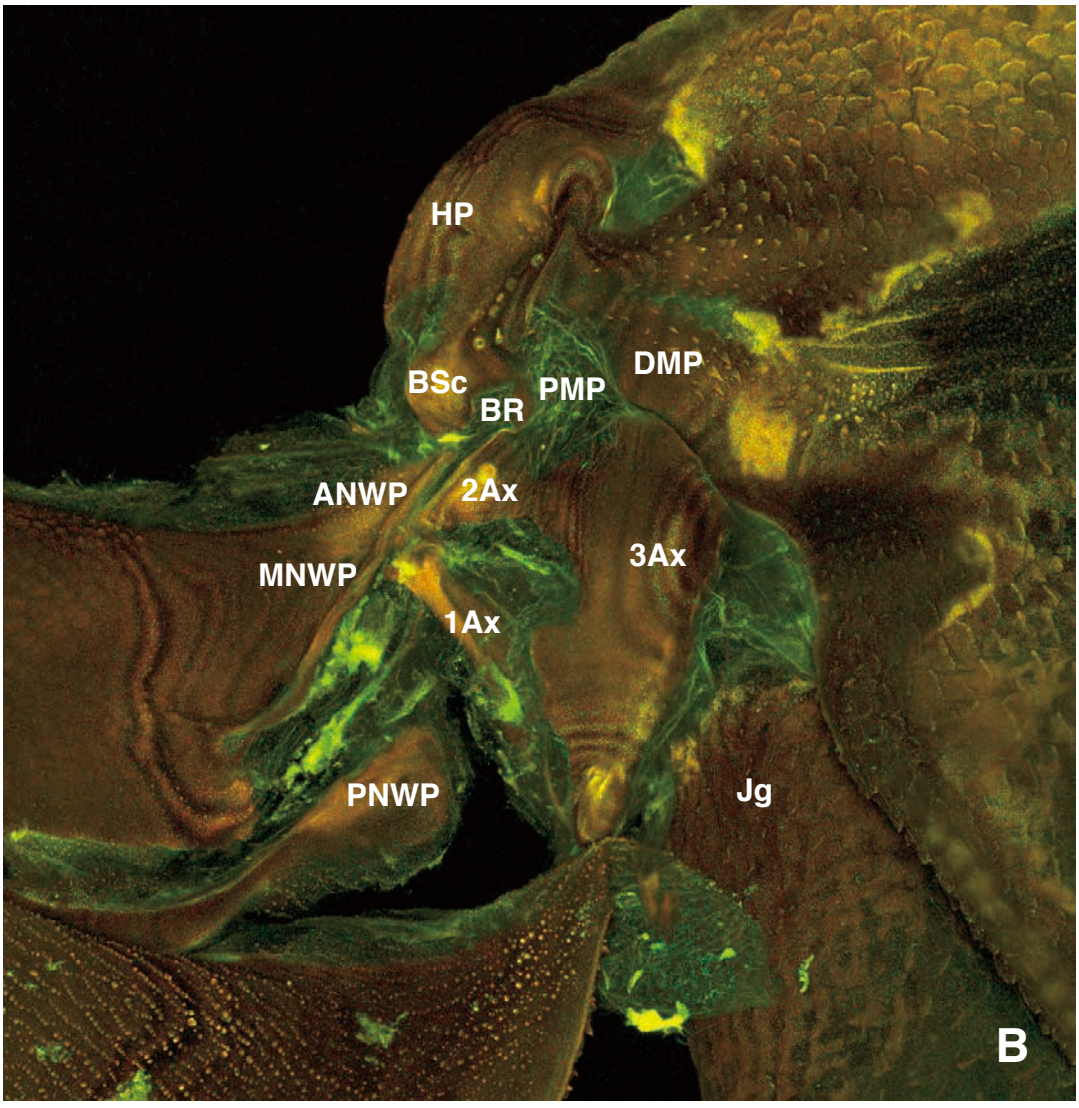
HP
BSc
BR
PMP
DMP
ANWP
2Ax
3Ax
MNWP
1Ax
PNWP
Jg
B

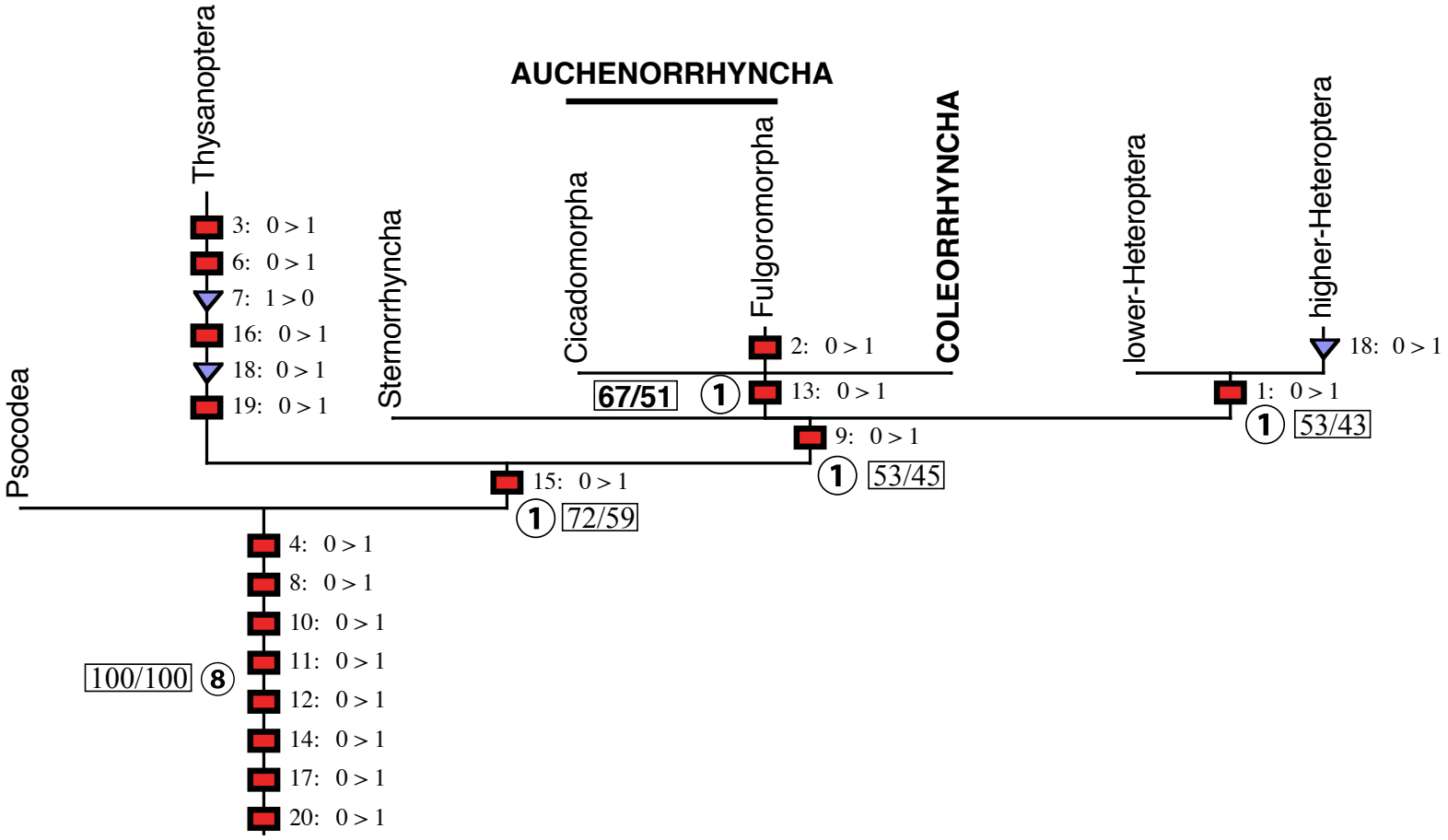
Thysanoptera
AUCHENORRHYNCHA
Cicadomorpha
Fulgoromorpha
COLEORRHYNCHA
lower-Heteroptera
higher-Heteroptera
Sternorrhyncha
Psocodea
3: 0 > 1
6: 0 > 1
7: 1 > 0
16: 0 > 1
18: 0 > 1
19: 0 > 1
2: 0 > 1
18: 0 > 1
67/51
1
13: 0 > 1
1: 0 > 1
1
53/43
9: 0 > 1
1
53/45
15: 0 > 1
1
72/59
4: 0 > 1
8: 0 > 1
10: 0 > 1
11: 0 > 1
100/100
8
12: 0 > 1
14: 0 > 1
17: 0 > 1
20: 0 > 1

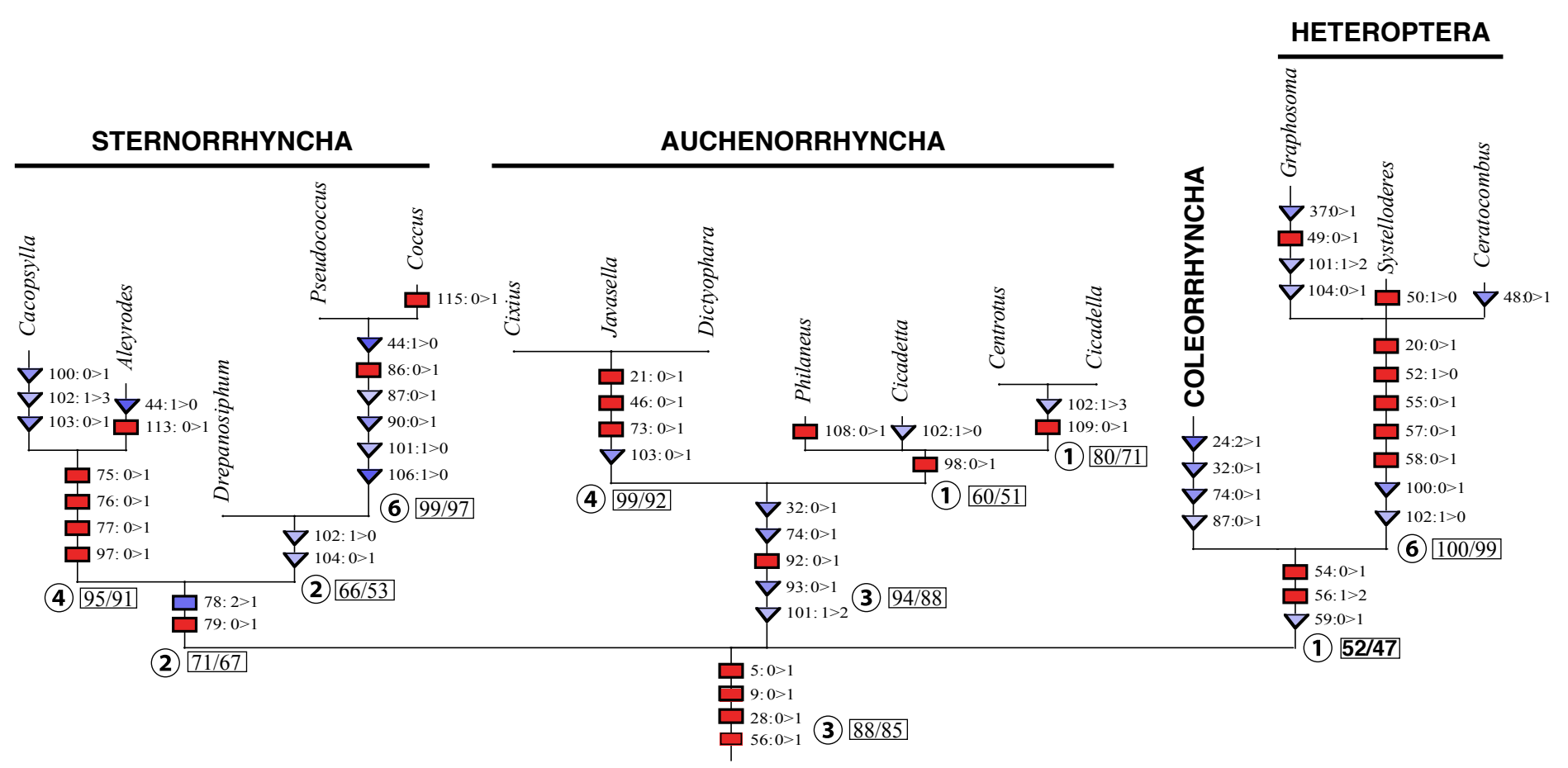
HETEROPTERA
STERNORRHYNCHA
AUCHENORRHYNCHA
COLEORRHYNCHA
Graphosoma
Systelloderes
Ceratocombus
Cacopsylla
Aleyrodes
Drepanosiphum
Pseudococcus
Coccus
Cixius
Javasella
Dictyophara
Philaneus
Cicadetta
Centrotus
Cicadella
37:0>1
49:0>1
101:1>2
104:0>1
50:1>0
48:0>1
20:0>1
52:1>0
55:0>1
57:0>1
58:0>1
100:0>1
102:1>0
6 100/99
24:2>1
32:0>1
74:0>1
87:0>1
54:0>1
56:1>2
59:0>1
1 52/47
100:0>1
102:1>3
103:0>1
44:1>0
113:0>1
75:0>1
76:0>1
77:0>1
97:0>1
4 95/91
78:2>1
79:0>1
2 71/67
102:1>0
104:0>1
2 66/53
115:0>1
44:1>0
86:0>1
87:0>1
90:0>1
101:1>0
106:1>0
6 99/97
21:0>1
46:0>1
73:0>1
103:0>1
4 99/92
108:0>1
102:1>0
98:0>1
1 60/51
102:1>3
109:0>1
1 80/71
32:0>1
74:0>1
92:0>1
93:0>1
101:1>2
3 94/88
5:0>1
9:0>1
28:0>1
56:0>1
3 88/85